JOINT EUROPEAN TORUS JET

JET-P(89)59

B.J. Green

JET Experimental Results

JET Experimental Results

B.J. Green

JET Joint Undertaking, Culham Science Centre, OX14 3DB, Abingdon, UK

Preprint of a paper to be submitted for publication in
Nuclear Energy Journal

ABSTRACT.

The Joint European Torus (JET) has demonstrated its ability to produce plasma with parameters (e.g. density, temperature and confinement time) closer to self-sustaining, thermonuclear conditions than any other tokamak. The increased energy confinement times (to greater than 1s) which have been obtained justify the extrapolation of tokamaks in size to JET. As a result of the investigation of new plasma parameter regimes, considerable knowledge has been obtained concerning plasma energy and particle transport, and methods have been found to reduce the problem of impurities and to provide refueling. Although there is an improved knowledge of high-temperature plasma behaviour, understanding is not yet complete. “Classical” theory is found to provide agreement with experiment in several situations. The degree of anomaly in other cases has been quantitatively examined by a variety of methods but does not appear to present an insuperable barrier to the achievement of reactor-relevant plasma conditions. Overall, the JET experimental results are very encouraging for the success of this research and they are tantalisingly close to fulfilling the original objective for this experiment.

1. Introduction

The essential objective of the JET experiment, established by the JET Design Team[1] and agreed by the partners in 1975, is : to obtain and study a plasma with conditions and dimensions approaching those needed in a thermonuclear reactor. These studies will be aimed at defining the parameters, the size and working conditions of a tokamak reactor. The realization of this objective involves four main areas of work :

(i) the study of the way plasma confinement properties scale as the dimensions and parameters approach those necessary for a fusion reactor,

(ii) the examination and control of the plasma-wall interaction and impurity influx under these conditions,

(iii) the demonstration of effective heating techniques, capable of producing high temperatures in JET in the presence of prevailing loss processes,

(iv) the study of alpha-particle production, confinement and subsequent interaction and heating i.e. the physics of a reacting plasma.

To accomplish the above, the JET experimental programme, which began in mid-1983, was divided into several Phases:

I	-	**OHMIC HEATING STUDIES**
II A & B	-	**ADDITIONAL HEATING STUDIES**
III A & B	-	**FULL POWER OPTIMISATION STUDIES**
IV	-	**DEUTERIUM - TRITIUM FUSION STUDIES**

Phase I

Phase I was completed by the end of September 1984 and involved operating JET at plasma currents up to about 3.7 MA. Maximum electron temperatures were in excess of 4 keV.*

Phase IIA

Phase II A was completed by December 1986 and involved plasma currents of up to 5 MA, three RF heating antennae delivering ion cyclotron resonance frequency (ICRF) heating power of up to 7 MW, and one neutral beam (NB) injection box which initially injected 65 keV hydrogen neutrals and was then converted to inject 80 keV deuterium neutrals at powers of up to 10 MW.

Also in this period, the four carbon-faced limiters, which bounded the outer plasma edge at the vessel mid-plane, were increased in number to eight and a significant fraction of metal surface of the vessel interior was protected by graphite tiles.

First experiments were conducted in magnetic configurations not limited by the carbon limiters; the so-called single X-point (with currents of up to 3 MA), and the so-called double X-point (with currents of up to 2.5 MA).

The application of up to 18 MW total heating power to the plasma increased peak temperatures, so that electron temperatures of up to 7.5 keV and ion temperatures of up to 10 keV were achieved. Unfortunately, a steady degradation of energy confinement with increasing additional heating power was observed.

* Plasma temperatures are typically quoted in (particle) energy equivalent units (keV). A temperature of 1 keV is equivalent to 11.4 x 10^6ºC.

Phase IIB

Phase IIB was completed by the end of September 1988 and involved a further increase in additional heating viz., a second neutral beam injection box (10 MW deuterium neutrals), and replacement of the three RF heating antennae by eight new systems. This allowed the application of a total additional heating power of more than 30 MW leading to high peak ion temperatures (in low density target plasmas) of more than 20 keV, but more typically to electron and ion temperatures of about 10 keV. The plasma current was increased to 7 MA in limiter-bounded plasmas and 5 MA in single X-point plasmas.

It is the aim of this paper to discuss the major results obtained in Phases I to IIB in terms of the studies (i) - (iii) above, which are involved in the realization of the objective of the JET experiment. The real study of alpha-particle production (study (iv) above) will be carried out in Phase IV following the successful completion of Phase III.

Discussion of the JET design and improvements in its performance are treated in a companion paper [2], while the future plans for JET and the implications of the JET results for the next experimental apparatus are discussed in another companion paper[3].

A worthwhile discussion of methods of measurement and errors is beyond the scope of this article and will not be attempted here. To gain a feel for the magnitude of experimental errors the reader is referred to paper.[4]

2. Scaling of Plasma Confinement

Scaling with Plasma Current

It should be appreciated that when JET was designed (1973/74) the typical dimensions of tokamaks were : minor radius 20 cm, major radius 70 to 100 cm, and plasma currents were typically several hundred kiloamperes for durations of several hundreds of milli-

seconds. The JET parameters[2] represent a large extrapolation from the 1973 tokamak values, nevertheless the basic improvement of energy confinement time with plasma current is confirmed. This can be seen clearly from the JET results in Fig.1. Nevertheless, at current values which reduce the edge safety factor q to the range of 3 to 2, this favourable current dependence disappears. The edge safety factor characterizes the twist of the confining magnetic field and its value is significant for the macroscopic stability of the plasma. A "cylindrical" approximation to its value in a torus is given by

$$q_{cyl} = \frac{5AB}{\pi RI}$$

where A is is the cross-sectional area of the plasma (in m^2), I is the plasma current (in megamperes), B is the toroidal field (in Tesla) and R is the plasma torus major radius (in m).

Low and High Confinement

Fig. 1 (a) shows the experimental results for the so-called L (low)-mode of confinement. However, in single or double X-point plasma configurations, there is a transition to an H (high)-mode of confinement induced by neutral beam injection heating. There appears to be a power threshold required for this transition which increases with magnetic field. Only recently has ion cyclotron frequency heating caused reproducible L to H transitions. In the H mode, energy confinement is two to three times greater than in the L mode, but still exhibits the same degradation with additional heating power (Fig. 1 (b)).

It should be noted that while L-mode operation is essentially steady-state, the periods of H-mode confinement (Fig. 2) are transient (up to 4 s duration so far), because the density (and radiation) increase uncontrollably. Under some circumstances edge-localized plasma instabilities do manage to reduce this density build-up.

Fusion Figure of Merit

The figure of merit for the approach of plasma parameters to reactor-relevant conditions is the product $\hat{n}_i \hat{T}_i \tau_E$ where $\hat{n}_i$ and $\hat{T}_i$ are the peak (reacting) ion density and temperature respectively and τ_E is the (global) energy confinement. JET has achieved the highest figure of merit value achieved, of about 3×10^{20} m^{-3}keVs in H-mode operation and a value of 2×10^{20} m^{-3}keVs in L-mode operation. The degradation of energy confinement with additional heating power is such that it almost exactly nullifies the increase in pressure with additional heating power, so that the figure of merit does not increase with additional heating.

The JET values of $\hat{n}_i \hat{T}_i \tau_E$ should be compared with a value of about 5×10^{21} m^{-3} keVs required for the achievement of the self-sustaining (or ignition) condition, and with the value of 2×10^{18} m^{-3}keVs achieved in the mid-1970's with the French tokamak TFR. This latter value was 10 times greater than the value achieved with the Soviet tokamak T3 in the late 1960's.

Scaling with Size

The scaling of energy confinement with plasma dimensions is more difficult to establish in one apparatus where the range of variation is very limited. Nevertheless, over the results of many different size tokamaks it appears to exist although perhaps not quite so strongly as the classical theory of particle and energy transport (based on Coulomb-collisions) would predict i.e. proportional to a^2 where a is a typical dimension for the minor plasma cross-section.

Scaling with Density

Energy confinement varies with density as $\sqrt{n}$ (n is the plasma particle number density) for ohmic discharges and those with low

additional heating power, but is essentially independent of n with large additional heating power discharges.

Improved Confinement

A general feature of tokamak plasma behaviour is the existence of internal disruption relaxations (the so-called sawtooth activity). This dominates the energy and particle transport within a certain plasma radius. Experiments in JET have shown that it is possible with additional heating to stabilize (for a time) their instabilities responsible for such sawteeth, with the result that a "monster" sawtooth is produced. Monster sawtooth durations of up to 3.2 s have been achieved (Fig 3). This stabilization leads to a moderate improvement in energy confinement (up to 20%) but will ultimately be useful for increasing the fusion figure of merit by peaking the density and temperature profiles.

"Improved" confinement regimes have been produced by ICRF heating in the plasma current-rise phase (thereby delaying the onset of sawteeth), and by the heating (neutral beams and/or ICRF) of plasmas with a peaked density profile formed by the injection of pellets of deuterium. Such improvements which have been achieved are modest (about 20%) and are transient.

Anomalous Transport

Plasma particle and energy transport outside the region dominated by sawtooth oscillations have been studied[4] and with the exception of the edge region (dominated by atomic processes e.g. radiation, recombination and ionization under the strong influence of plasma-wall interactions), appears to be anomalous. This means that the transport is larger than that based on Coulomb-collisions including particles trapped in the variation of the toroidal magnetic field in major radius (the basis for the so-called neo-classical theory). In fact, local analysis of profile data for a fairly wide range of JET plasmas

shows that the ratio of the electron thermal conductivity to the electron particle diffusion coefficient is about 7.2 (±3.0). For H-mode plasmas the ratio of ion thermal conductivity to electron thermal conductivity lies in the range 0.3 to 1.0. The large value of the ratio of thermal conductivity to particle diffusion coefficient suggests that micro-magnetic stochasticity, rather than electrostatic-turbulence-induced convection may be the key mechanism in anomalous transport[5].

Classical Behaviour

While the plasma thermal conductivity appears anomalous, the plasma electrical resistivity appears to be neo-classical under certain conditions[6].

Near the end of the current flat-top, the classical and neo-classical values of the plasma resistivity (η_S and η^* respectively) are calculated using the measured plasma profiles. A uniform value of the plasma effective charge number Z_{eff} is assumed and its value is taken from a measurement of visible Bremsstrahlung.

These two values are compared with the actual value h_{eff} which is obtained from the ratio of surface-averaged electric field to current density. The η^*/η_S ratio usually lies in the range 1.5 to 2. The neoclassical values are much closer to the actual values (Fig. 4).

A further study of the electrical resistivity was carried out by examining the field penetration following a current ramp say from 1 to 2 MA. Equilibrium calculations allowed the flux, toroidal current density and toroidal electrical field within the plasma to be calculated. This allowed the resistivity h_{eff} to be calculated as a function of space and time. A comparison with h^* and h_S was made, and once again the neoclassical value fitted best.

Another neoclassical effect which has been observed is that of the bootstrap current. This current is essentially due to the presence

of a population of trapped particles in a region where a plasma pressure gradient exists. Hence it is peaked off-axis and is largest in the region of the steepest pressure gradient. This current dominates other effects (e.g. neutral beam-driven currents) in H-mode plasmas and bootstrap currents of up to 0.8 MA (in a total plasma current of 3 MA) have been observed, in broad agreement with theory.

3. *Impurities*

For a reactor-plasma mixture of hydrogen isotopes (e.g. deuterium and tritium), non-hydrogenic material (e.g. helium, carbon, oxygen, metals etc) are impurities and have a deleterious effect on performance because :

a) the impurities dilute the concentration of reacting ions (n_i) thereby reducing fusion power. The ratio of ion density to electron density is :

$$\frac{n_i}{n_e} = (Z_i - Z_{eff})/(Z_i - 1)$$

where Z_i is charge number of the principal impurity and Z_{eff} is the effective charge number of all impurities ($=\Sigma n_i Z_i^2 / \Sigma n_i Z_i$).

(b) the impurities enhance the radiation losses (Bremsstrahlung, line and recombination radiation) i.e. they degrade the energy confinement.

Classical transport theory predicts that the impurities will accumulate in the plasma centre thereby exacerbating a) and possibly b).

(c) The impurities limit the density achieved (see section 4).

Knowledge of impurity concentration is based mainly on the analysis of resonance line intensities in the visible vacuum ultra violet (VUV) and information from soft X-ray emission.

The main impurity radiation loss in JET is due to carbon and oxygen and originates mainly from the plasma edge. The effect of metals from the wall has been reduced by protecting much of the wall with carbon tiles. Nickel (the most important metal impurity) from the ICRF antenna screens enters the plasma during high power ICRF heating. With neutral beam heating and pellet injection the relative impurity fractions (and Z_{eff}) are reduced.

In normal limiter-bounded discharges the anomalous particle transport prevents accumulation of impurities. However in long pulses (Fig.5) this classical effect becomes apparent and in this case, the dominant impurity was carbon. Similarly, H-mode phases (Fig.2) revert to L-mode following a density and impurity build-up as a result of improved particle confinement, but curiously, this effect is not seen in monster sawteeth. Peaked density profiles produced by pellet injection exhibit impurity accumulation in the plasma core.

Control of Impurities

To attempt to control the impurities in JET the following measures have been applied:

(a) Glow Discharge Cleaning.

(b) Pulse Discharge Cleaning.

(c) Bakeout and hot vessel walls.

(d) Low Z material for in-vessel elements facing the plasma.

(e) Carbonization.

(f) Density screening.

The wall conditioning methods tried were (a) - (e) above. The mechanism of impurity removal for (a) and (b) is the chemical reaction of low Z impurities with atomic hydrogen to form volatile compounds which are then pumped away.

The methods (a) to (e) are briefly reviewed in the following: For Glow Discharge Cleaning (GDC) two electrodes situated in vessel ports are used. Gas is continuously introduced at typically 5×10^{-3} mbar and a DC current of about 8 A is maintained between the electrodes (anodes) and the vessel (cathode). The effects of GDC are mixed:

(i) there is considerable gas (hydrogen or deuterium) absorbed in the wall/limiter surface which leads to strongly enhanced recycling in subsequent tokamak discharges. In some cases this effect has led to difficulty in achieving a sustained breakdown in the first few discharges following GDC (in particular with carbonisation - see below).

(ii) there is a strong suspicion that GDC causes the migration of some metal from the wall near the electrodes to the limiters. This metal can be easily released in subsequent high power tokamak discharges.

(iii) the plasma density limit achieved in reference discharges after GDC is a measure for the level of impurities which are present. This density limit increases somewhat (i.e. impurity concentration is decreased) following GDC, but the effect is not dramatic and is complicated by (i).

decreased) following GDC, but the effect is not dramatic and is complicated by (i).

Pulse discharge cleaning (PDC) : in mid 1984, 12000 short hydrogen pulses were performed with :

Toroidal field = 0.15 T

Plasma current = 30-40 kA

Plasma duration = 0.5 s

Pulse frequency = 3-4 per min

The influxes of carbon and oxygen in reference discharges were somewhat lower after PDC but the chromium level increased. The overall effect of PDC left Z_{eff} essentially unaltered and the radiation power loss remained about 80% Ohmic input power. As PDC did not improve the impurity situation significantly it has not been repeated.

After the vessel has been opened (for in-vessel installation etc), it is pumped at high temperature (up to 350ºC) to desorb volatile impurities (bakeout). Tokamak operation is normally carried out with the double-walled vessel at 300ºC while the single-walled ports are maintained at about 150ºC. No systematic study has been performed on the effects on operation of varying the vessel temperature. Nevertheless a typical base pressure is 10^{-7} mbar hydrogen with 10^{-9} mbar of residual impurities at a vessel temperature of 300ºC.

Original operation of JET was with an inconel (metal) wall surface facing the plasma and four discrete graphite limiters. In an effort to reduce metallic (high atomic number Z) contamination which arose mostly as a result of disruptive discharges terminating on the inner wall, graphite tiles were installed to cover this wall to a height of 1 m above and below the mid-plane. This was successful in reducing the metallic impurities. Subsequently, the amount of installed graphite tiling has been increased to cover most of the vessel elements facing

the plasma. Indeed, the graphite limiters have now been replaced by two toroidal (belt) limiters placed at the same distance above and below the mid-plane, and special protective tiles have been strategically placed to cope with neutral beam shine-through and localised energy deposition at the X-points.

The covering of a significant part of the inner surface by carbon reduces the amount of metal which reaches the plasma and hence the damaging radiation loss from the hot plasma centre. Carbon now becomes a significant impurity but the associated radiation loss tends to be confined to the cooler plasma edge, which is an energetically more favourable situation than for heavy metal impurities.

Carbonization or carbidization is the name given to the process whereby the inner surfaces are covered by a layer of carbon or carbides. This is achieved by glow discharge cleaning in a mixture of hydrogen and methane (CH_4). After 'light' carbonization (12% CH_4, 6 hr GDC) the metal radiation drops by a factor 5 and the radiated power drops from 70% to 50% of the Ohmic input. The effects of this carbonization are lost after about 20 tokamak pulses. After heavy carbonization (17% CH_4, 48 hr GDC), metal radiation drops by a factor 100. The effects of this carbonization are lost after about 200 pulses (Fig. 6). The reduction in impurity level modifies the radial power balance and increases the ohmic density limit somewhat (about 10%).

The effective charge number of the plasma is reduced as the average density of plasma increases (Fig. 7). The metal impurity influx is more effectively screened at high density, but the oxygen impurity is relatively insensitive to plasma density but more dependant on the state of the vessel. At high plasma density, radiation losses were mainly caused by carbon and oxygen. Z_{eff} usually ranges between 2 and 3 for an average electron density of 3×10^{19} m^{-3}, but approached 1

for a time duration of about 0.5 s after the injection of a deuterium pellet.

At higher density the plasma temperatures are reduced which leads to a lower sputtering yield of metals and carbon from the limiter. The oxygen content is roughly independent of density.

When a magnetic separatrix is formed there is a reduction in carbon content compared with similar limiter discharges. However, this leads to only a minor reduction in Z_{eff}. Neutral beam heating leads to an increase in carbon concentrations in such plasmas which is in contrast to the decreased carbon concentration for NB heating in limiter discharges.

4. *Plasma Heating*

With the continual increase in the additional heating power applied (NB up to 21 MW and RF up to 16 MW), the plasma temperatures have also increased. For example (Fig. 8) both electron (T_e) and ion temperatures (T_i) greater than 10 keV have been maintained for about 2 s at a mean density of somewhat more than 10^{19} m^{-3}. Central ion and electron temperatures in excess of 5 keV have been sustained for 20 s by 6 MW ICRF heating (Fig. 5).

For plasma discharges where the density is deliberately reduced (the inner-wall discharges where the carbon tiles conditioned by the GDC and subsequently by He discharges provide a very effective 'pump'), it is possible to produce "hot-ion" plasmas i.e. where the ion temperature (23 keV) is much higher than the electron temperature (8-12 keV).

Similarly, good-density "control" is found in the double X-point configuration which allows high temperatures to be achieved viz., T_i = 18 keV with NB, and T_e = 12 keV with ICRF. The highest

fusion parameter achieved was with an H-mode plasma of temperature in excess of 5 keV.

ICRF Heating

High-power ICRF heating has been particularly successful in heating limiter plasmas. High central temperatures ($T_e \approx 11$ keV, $T_i \approx 8$ keV) have been achieved in monster sawteeth. ICRF heating at the fundamental cyclotron resonance of a minority ion species is effective in producing a high ion energy population which then transfers energy to electrons in agreement with classical theory. There is also some direct electron heating, up to 30% for ^3He minority but only up to 10% for an H minority (in deuterium). In the ^3He minority case there is significant non-thermal fusion of deuterium and helium leading to the production of up to 60 kW charged-particle fusion reaction products (for 12 MW ICRF) arising from:

$$^2D + {}^3He \rightarrow p\ (14.7\ MeV) + {}^4He\ (3.7\ MeV)$$

The fusion rate achieved is $2 \times 10^{16}\ s^{-1}$.

Combined ICRF/NB heating can be arranged so that the ICRF couples energy at the second harmonic of deuterium to enhance the deuterium-deuterium (D-D) fusion reaction. The tritons which result from (D-D) fusion are found to slow down according to classical theory. Peaked density profiles produced by pellet injection can be effectively (re-)heated by ICRF which has a spatially localized energy deposition (about the cyclotron resonance surface). High fusion indices ($2.2 \times 10^{20}\ m^{-3}$ keVs) have been achieved.

This ^3He minority heating simulates heating of a D minority in a tritium plasma and thus several features of the physics of alpha particles (^4He) produced in D-T fusion have already been studied (see Table 1). Behaviour is broadly as expected. The corresponding D-T scheme could produce a fusion power of the order of several MW.

NB Heating

NB Heating leads to ion temperatures greater than or equal to the electron temperatures. The slowing down of high energy deuterium beam ions normally dominates the D-D thermonuclear fusion by beam-plasma and beam-beam contributions. This leads to the achievement of values for the power amplification ratio Q (ratio of fusion power output to plasma heating power input) up to 6×10^{-4}. Such performance when converted to D-T operation gives Q values of about 0.25.

Maximum neutron production rates of in excess of $10^{16}\ s^{-1}$ have been achieved.

Beam driven currents of up to 0.5 MA, which are due to the injected fast ion current (modified by particle trapping in the inhomogeneous confining magnetic field), have been observed. Such currents tend to dominate bootstrap currents in low density plasmas and are rather peaked.

Density Limits

As in other tokamaks, the plasma density in JET is limited. For OH discharges (before carbonization) the plasma density limit (n_L) was

$$n_L\ (m^{-3}) = 1.2 \times 10^{20}\ B/(Rq_{cyl})$$

where q_{cyl} is the cylindrical approximation to the edge safety factor, B is the toroidal field (in Tesla), and R is the plasma torus major radius (in m).

The high density limit depends on the plasma purity (it was increased by about 10% after carbonization), and on the power input. Large amounts of neutral beam heating push the density to twice the Ohmic heating (OH) density limit (Fig. 9). This shows that internal fueling of the discharge is important because RF power does not have the same effect. This is reinforced by the results obtained with pellet

injection (Fig. 9(a)) where peak density values of 2×10^{20} m^{-3} have been (transiently) obtained.

The density limits are of two kinds:

(a) a low q limit

(b) a high density limit

An attempt to break through these limits results in major disruptions. This disruption is a dramatic event in which plasma confinement is suddenly destroyed (energy loss in several 100 ms) followed by a complete loss of current in times of the order of 10 ms). Such disruptions not only limit the range of operation but they lead to large mechanical stresses and heat loads on the vessel.

The high density limit disruption is invariably preceded by a peaking of the temperature (current) profile (a "radiative" collapse). In this disruption the radiated power is roughly equal to the total input power.

5. *Conclusions*

1. Although details of particle and energy transport are not yet understood, JET has already achieved a significant level of plasma confinement which it appears possible to improve . It is encouraging that at the thermonuclear temperatures achieved, no strongly temperature-dependent losses are observed. A broad range of results has been successfully modelled so as to permit an extrapolation of the plasma confinement behaviour to optimised JET operation and that of future machines. On this basis tokamak reactor-like energy confinement can be achieved.

2. Improvements in plasma purity have been achieved primarily with the low protective covering of the metallic vessel surface facing the plasma. Nevertheless, it is clear that further gains

must be made. This is probably the area of most concern to the successful completion of the programme.

3. Both neutral beam and ion cyclotron resonance frequency heating have been successful in achieving reactor-relevant plasma temperatures. The advantages and disadvantages of these methods appear to be well understood.

4. The highest fusion product values (2 - 3 x 10^{20} keV m^{-3} s) have been achieved in different discharge types (H-mode, pellet-fuelled, hot-ion). Thus, conditions have been achieved corresponding to a power amplification factor in a 50:50 deuterium-tritium mixture of about 0.25 including both thermonuclear and non-thermonuclear contributions. Some improvement in this performance appears possible and this should allow JET to successfully pursue the study of alpha-particle production, confinement and heating. Some aspects of alpha-particle physics have already been simulated by the RF heating of ^{3}He minority ions in a D plasma. The behaviour is broadly as expected.

5. Agreement of theory with experiment for several aspects of JET plasma performance is improving, in particular for some neoclassical effects (electrical resistivity, the bootstrap current, the beam-driven current and the slowing-down of fast particles).

6. Full exploitation of the existing machine and its associated systems should allow for improvements in performance (e.g.sustained peaked profiles, H-modes, and monsters, and control of Z_{eff} and disruptions). Planned technical developments[3] should allow further gains and hence give increased confidence that JET will successfully complete its programme thereby defining the parameters of the next-step fusion device with which the technological problems of a fusion reactor will be studied and, hopefully, solved.

References

1. "The JET Project : Design Proposal of the Joint European Torus", EUR-5516e (EUR-JET-R5)Commission of the European Communities.

2. Bertolini E, "JET Design, Construction and Performance", this issue.

3. Rebut P-H, " Future Plans for JET and Ideas for a Post-JET Machine", this issue.

4. Cheetham A.D. et al, "Measurements of Correlations between Thermal and Particle Transport in JET", 12th IAEA Conference on Plasma Physics and Controlled Nuclear Fusion Research (Nice, France 1988), to be published in Nuclear Fusion Supplement, IAEA-CN-50/I-2-2.

5. Rebut P-H. et al, "The Critical Temperature Gradient Model of Plasma Transport: Applications to JET and future Tokamaks", 12th IAEA Conference on Plasma Physics and Controlled Nuclear Fusion Research (Nice, France 1988), to be published in Nuclear Fusion Supplement, IAEA-CN-50/D-4-1.

6. Bickerton R.J., Taroni A, Watkins M.L, Wesson J, "Comparison between Experiment and Theory" JET-P (86) 28.

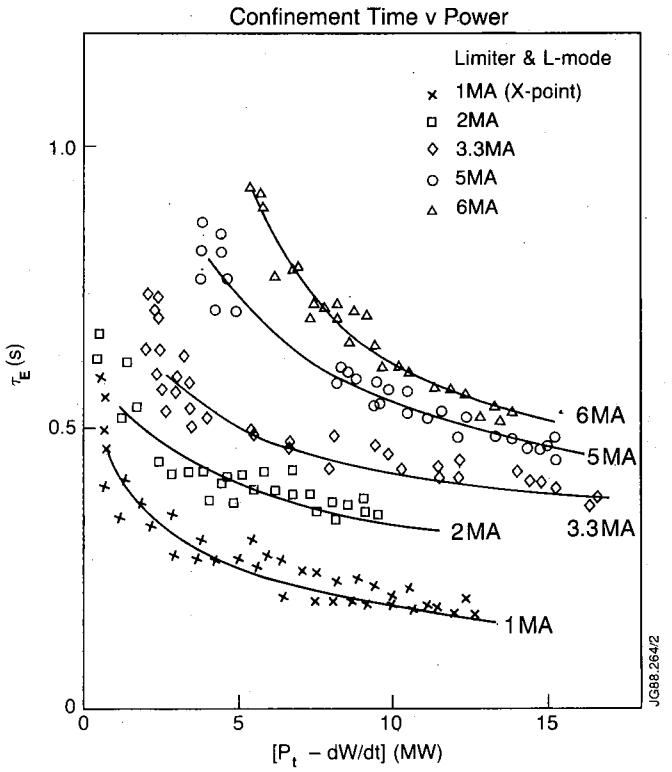

Fig. 1(a) L-mode confinement time τ_E data versus input power showing degradation with power. The beneficial effect of plasma current is clearly seen.

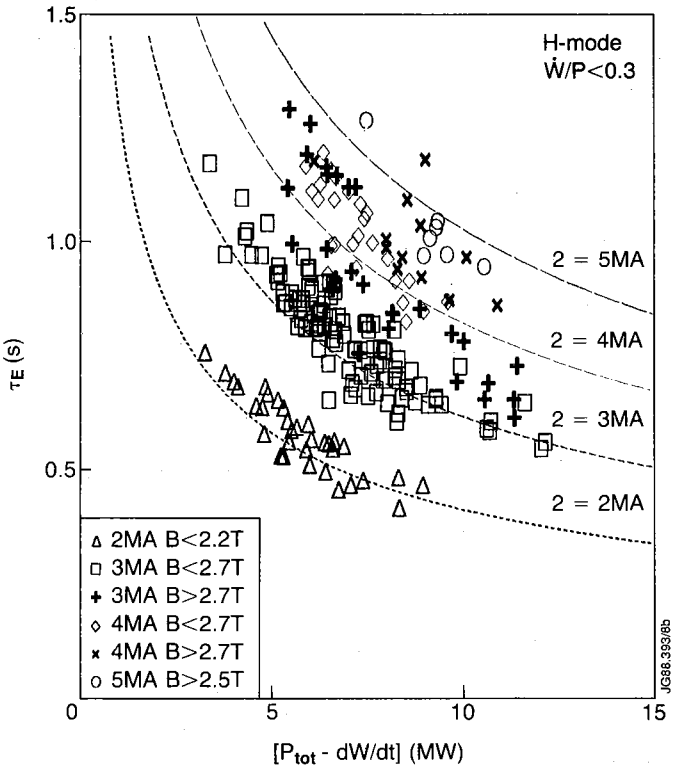

Fig. 1(b) H-mode confinement time τ_E data versus input power showing clear degradation with power. However confinement is improved by a factor of 2 to 3 over the corresponding L-mode case.

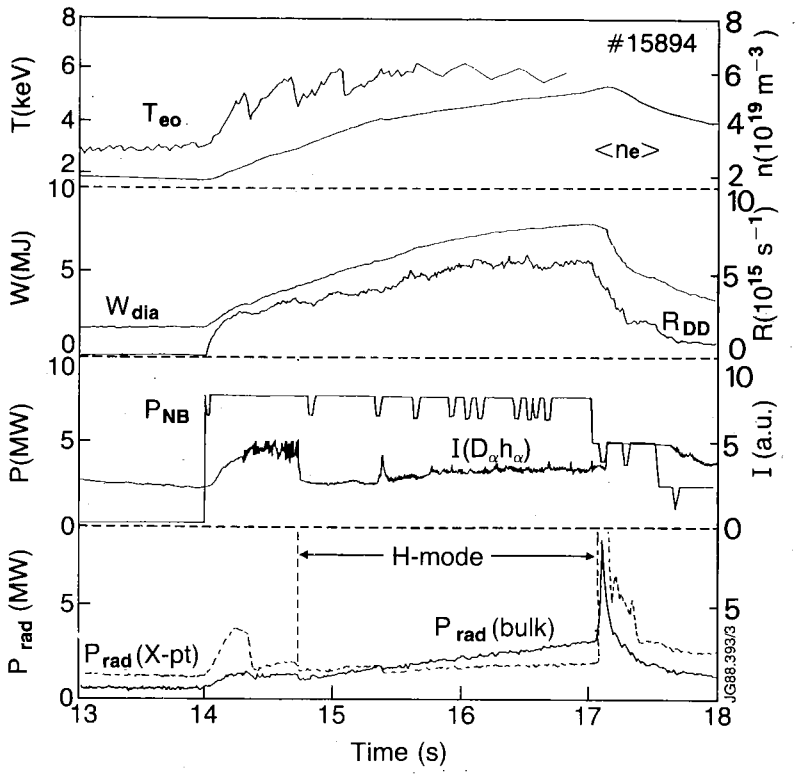

Fig. 2 Time evolution of electron temperature on axis T_{eo}, volume averaged electron density $<n_e>$, total plasma energy W_{dia}, total reaction rate R_{DD}, neutral beam power P_{NB}, $D\alpha$ intensity I($D\alpha$), bulk radiation P_{RAD} (bulk) and X-point radiation P_{RAD} (X-point) for a 3 MA H-mode discharge.

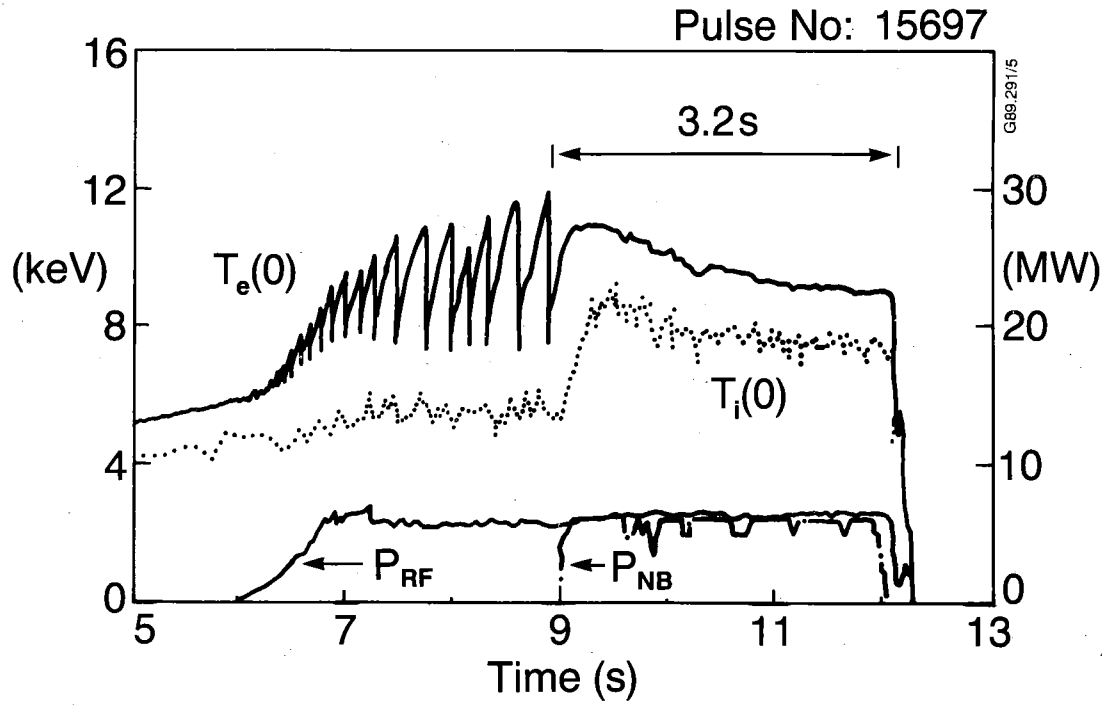

Fig. 3 Behaviour of central electron and ion temperature showing the longest period of sawtooth stabilization observed.

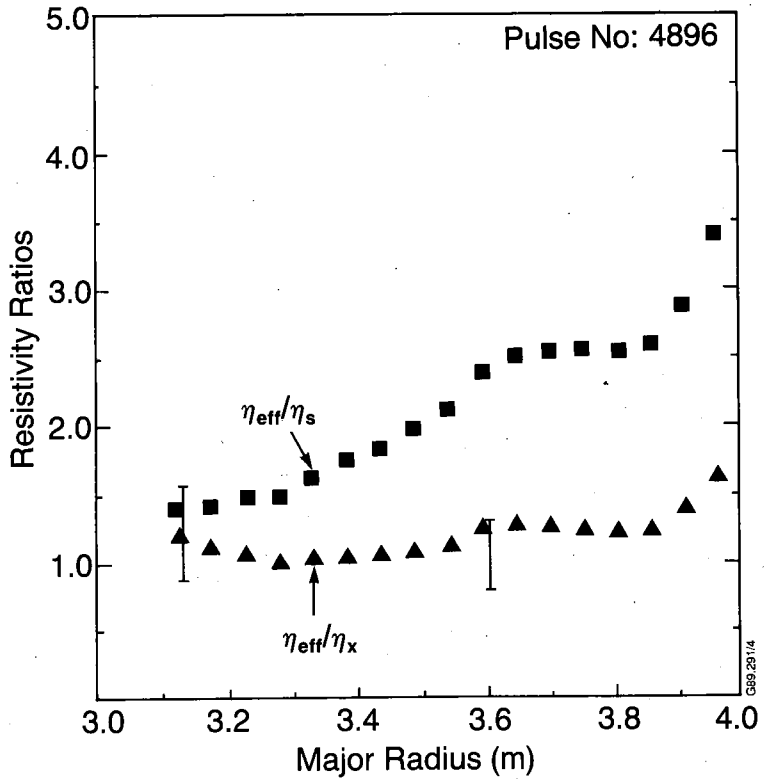

Fig. 4 The ratios of η_{eff}/η_s and η_{eff}/η^* plotted versus major radius at t=7s.

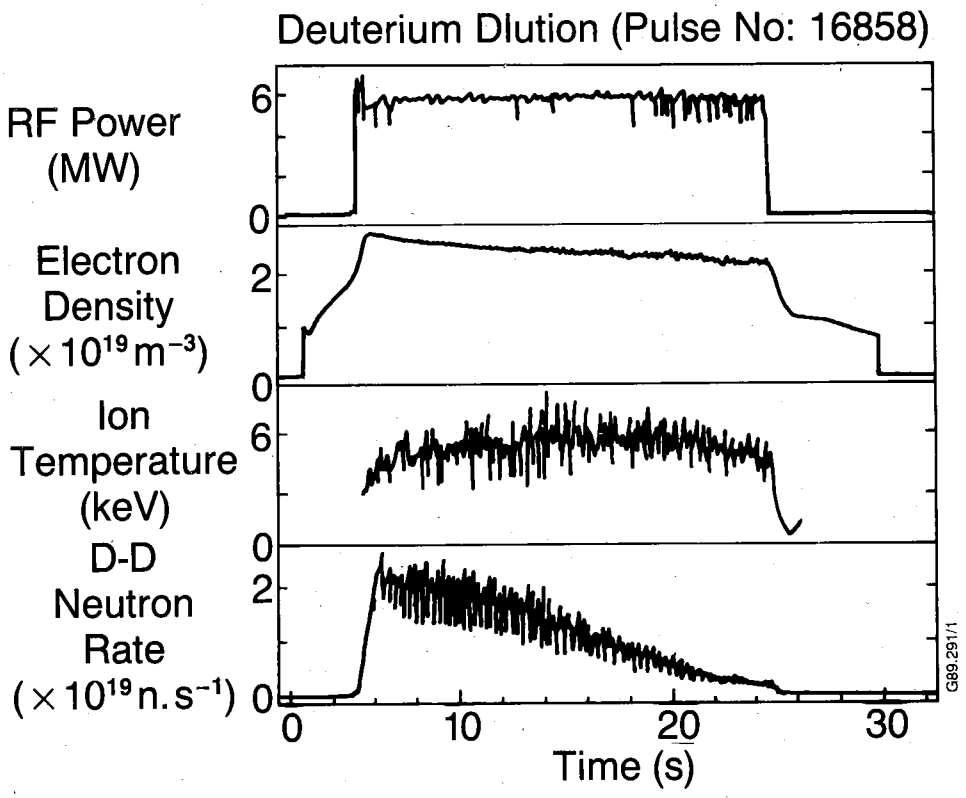

Fig. 5 Deuterium dilation by central impurity accumulation Pulse 16858.

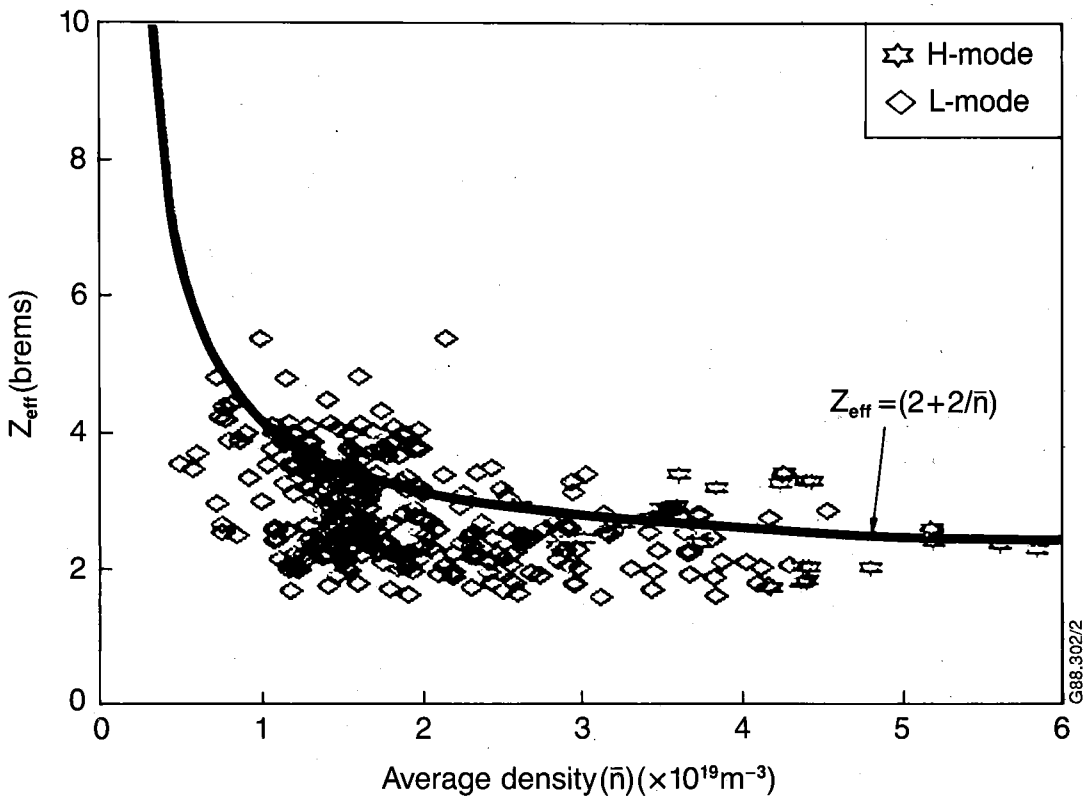

Fig. 6 Intensities of selected VUV impurity lines (for $n=2\times10^{19}\,m^{-3}$) demonstrating the respective impurity behaviour after light and heavy carbonization.

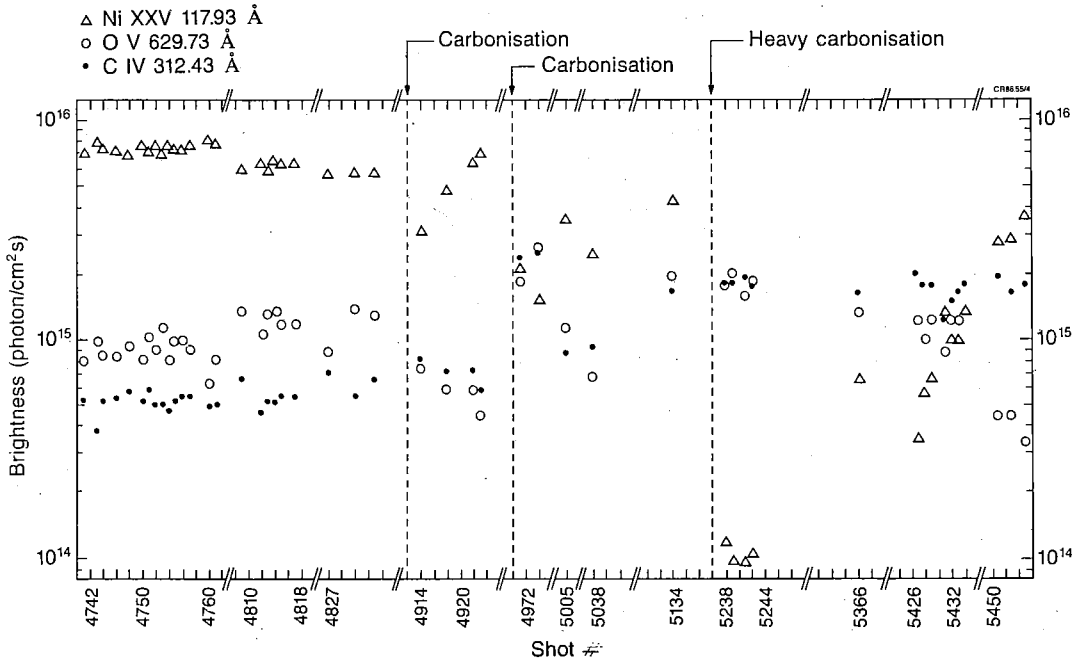

Fig. 7 Effective ion charge Z_{eff} versus average density for JET discharges. H-modes are identified separately.

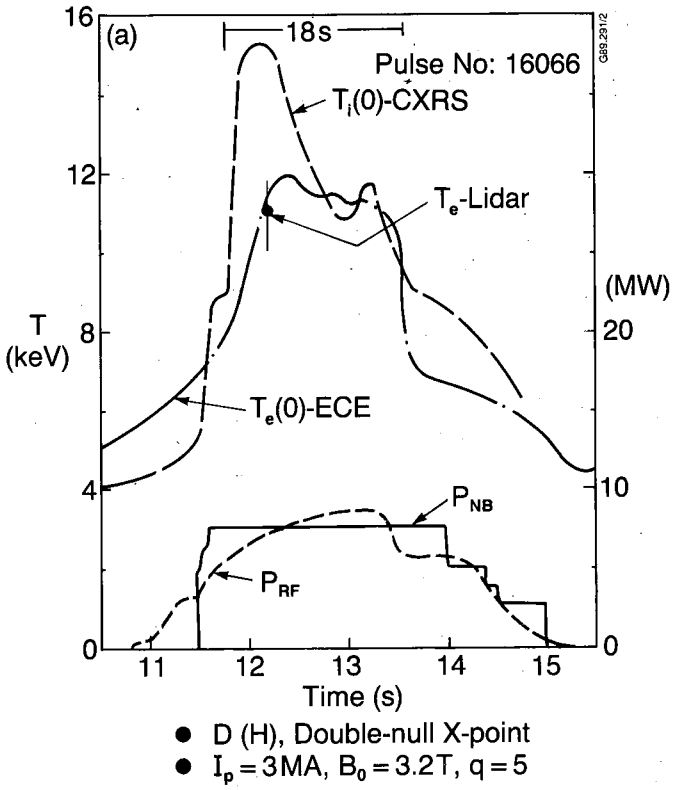

Fig. 8(a) Peak electron and ion temperature as a function of time during RF & NB heating.

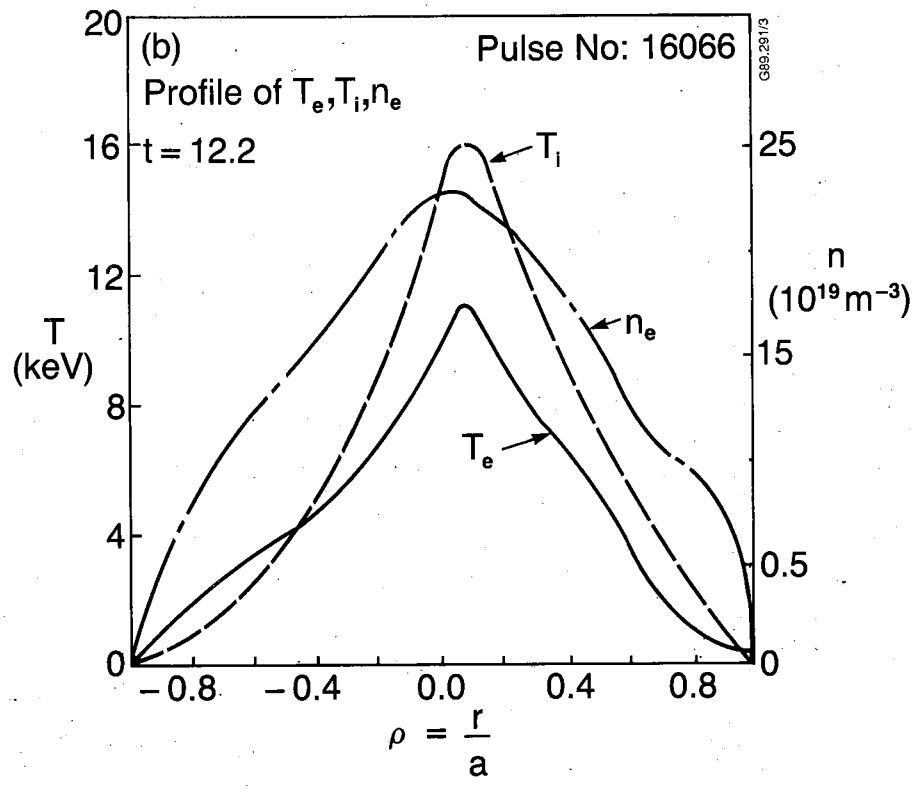

Fig. 8(b) Density and electron and ion temperature profiles at 12.2s for the same pulse as (a).

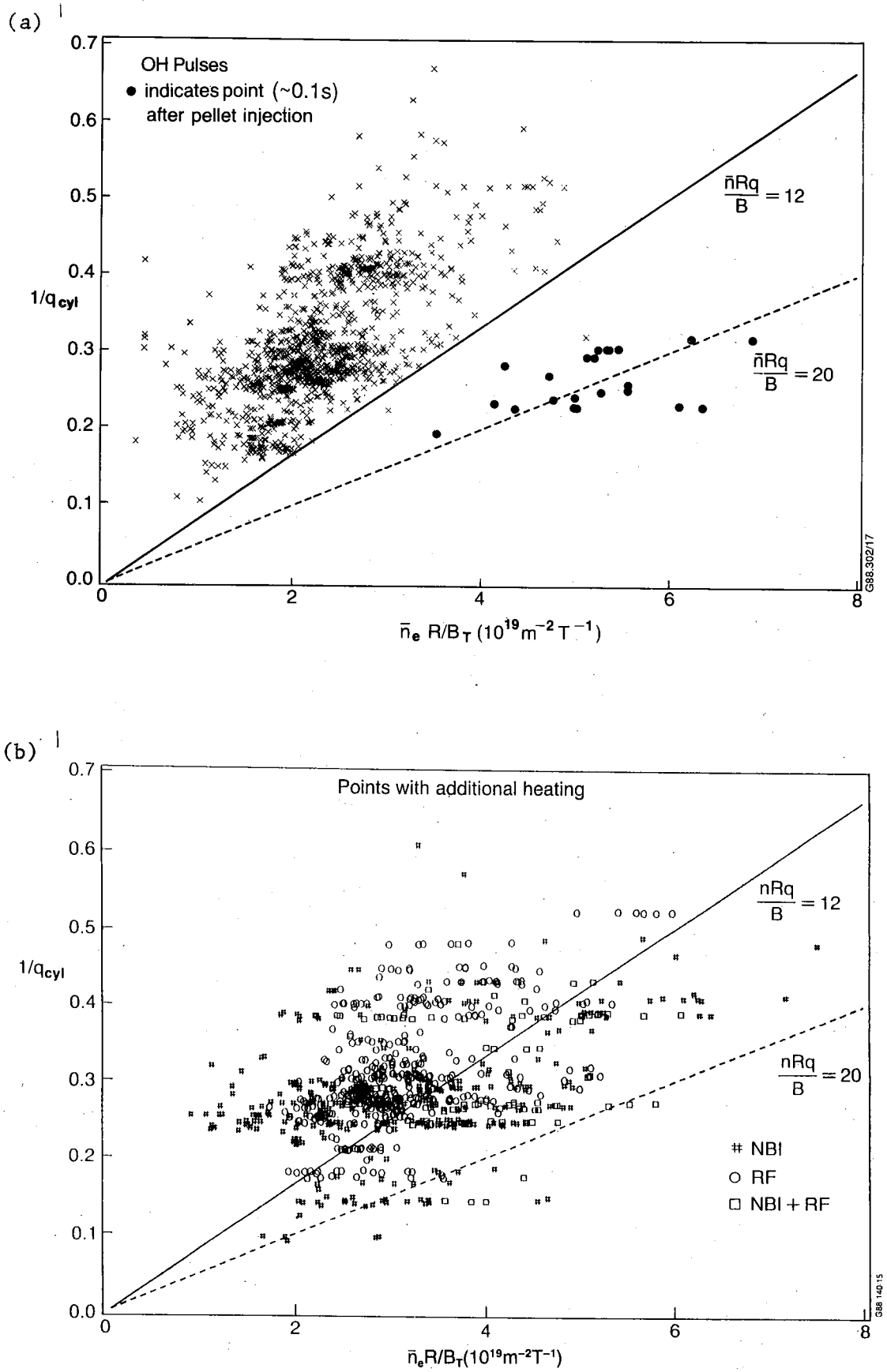

Fig. 9 Normalized plasma current $1/q_c$ versus normalized density $n\ R/B_T$ for non-disrupting discharges. (a) with ohmic heating (b) with additional heating.